

Feedback modulation of cholesterol metabolism by the lipid-responsive non-coding RNA *LeXis*

Tamer Sallam^{1,2*}, Marius C. Jones^{1*}, Thomas Gilliland¹, Li Zhang¹, Xiaohui Wu^{1,2}, Ascia Eskin³, Jaspreet Sandhu¹, David Casero¹, Thomas Q. de Aguiar Vallim², Cynthia Hong¹, Melanie Katz⁴, Richard Lee⁴, Julian Whitelegge⁵ & Peter Tontonoz¹

Liver X receptors (LXRs) are transcriptional regulators of cellular and systemic cholesterol homeostasis. Under conditions of excess cholesterol, LXR activation induces the expression of several genes involved in cholesterol efflux¹, facilitates cholesterol esterification by promoting fatty acid synthesis², and inhibits cholesterol uptake by the low-density lipoprotein receptor³. The fact that sterol content is maintained in a narrow range in most cell types and in the organism as a whole suggests that extensive crosstalk between regulatory pathways must exist. However, the molecular mechanisms that integrate LXRs with other lipid metabolic pathways are incompletely understood. Here we show that ligand activation of LXRs in mouse liver not only promotes cholesterol efflux, but also simultaneously inhibits cholesterol biosynthesis. We further identify the long non-coding RNA *LeXis* as a mediator of this effect. Hepatic *LeXis* expression is robustly induced in response to a Western diet (high in fat and cholesterol) or to pharmacological LXR activation. Raising or lowering *LeXis* levels in the liver affects the expression of genes involved in cholesterol biosynthesis and alters the cholesterol levels in the liver and plasma. *LeXis* interacts with and affects the DNA interactions of RALY, a heterogeneous ribonucleoprotein that acts as a transcriptional cofactor for cholesterol biosynthetic genes in the mouse liver. These findings outline a regulatory role for a non-coding RNA in lipid metabolism and advance our understanding of the mechanisms that coordinate sterol homeostasis.

It is well established that the cholesterol biosynthetic pathway is downregulated under conditions in which sterols are abundant through the inhibition of sterol regulatory element-binding protein (SREBP) processing⁴. Notably, however, under conditions in which hepatic cholesterol content was not enriched, activation of LXRs with the selective synthetic agonist GW3965 also acutely suppressed the expression of sterol synthesis genes in mouse liver (Fig. 1a and Extended Data Fig. 1a). The effect could not be explained by changes in intracellular cholesterol levels, as LXR activation has been shown to lower hepatic cholesterol content⁵, which would lead to upregulation of the SREBP-2 pathway.

To investigate the mechanism by which LXRs suppress cholesterol biosynthesis, we performed genome-wide transcriptional profiling on primary mouse hepatocytes treated with vehicle or GW3965 (Extended Data Fig. 1b). The most robustly induced gene in our RNA-sequencing (RNA-seq) analysis was a predicted non-coding RNA annotated as 4930412L05Rik (Extended Data Fig. 1c). Parallel profiling of non-coding and protein-coding transcripts using microarrays also identified 4930412L05Rik as the highest induced transcript (Extended Data Fig. 1d). We named this transcript *LeXis* (liver-expressed LXR-induced sequence). Notably, the *LeXis* gene locus lies in close proximity to the canonical LXR target gene *Abca1* in mouse. Analysis of chromatin structure from The ENCODE Project^{6,7} indicated that *LeXis* and *Abca1* were distinct genes with separate promoters

(Fig. 1b). We defined the transcripts produced from the *LeXis* gene using rapid amplification of complementary DNA ends (RACE) (Extended Data Fig. 2). *LeXis* and *Abca1* were induced by LXR and retinoid X receptor (RXR) agonists (LG268 and GW3965, respectively) in primary hepatocytes in an LXR-dependent manner (Fig. 1c and Extended Data Fig. 3a). *LeXis* was induced in *LXRα*^{-/-} and *LXRβ*^{-/-} (also known as *Nr1h3*^{-/-} and *Nr1h2*^{-/-}, respectively) hepatocytes, indicating that both LXR isotypes are capable of regulating *LeXis* (Extended Data Fig. 3b). Induction of *LeXis* was not sensitive to the protein synthesis inhibitor cycloheximide, and was not dependent on SREBPs, since 25-hydroxycholesterol (which blocks SREBP processing) also induced *LeXis* (Extended Data Fig. 3c, d).

Administration of GW3965 to mice induced the expression of *LeXis* in several metabolically active tissues (Fig. 1d and Extended Data Fig. 3e). We also observed a prominent, LXR-dependent induction of *LeXis* expression in response to Western diet feeding, consistent with a potential role for *LeXis* in the response to cholesterol excess (Fig. 1e). Despite being physically adjacent, the *LeXis* and *Abca1* loci are regulated independently. *LeXis* was neither expressed at baseline nor induced by LXR in mouse peritoneal macrophages, a cell type in which *Abca1* expression is prominent (Fig. 1f). A luciferase reporter containing the *LeXis* promoter was induced by LXR and RXR in co-transfection assays (Extended Data Fig. 3f), and we identified an LXR-response element within the *LeXis* promoter region that was bound by LXRα in chromatin immunoprecipitation and quantitative PCR (ChIP-qPCR) assays (Extended Data Fig. 3g). The coding potential calculator and coding-non-coding index algorithms predict low coding potential of *LeXis* (Extended Data Fig. 3h, i). In addition, we found no evidence of production of a protein product from *LeXis* using *in vitro* transcription-translation assays (Extended Data Fig. 3j).

To explore the function of *LeXis* *in vivo*, we transduced mice with adenoviral vectors encoding green fluorescent protein (GFP) control or *LeXis* (Fig. 2a and Extended Data Fig. 4a). Remarkably, *LeXis* expression decreased serum cholesterol, but not triglycerides, in chow-fed C57BL/6 mice (Fig. 2a, b). No differences in liver function tests were observed between the two groups, and there was no evidence of ER stress or inflammation (Fig. 2b and Extended Data Fig. 4b, c). Fractionation of lipoproteins revealed reduced cholesterol in both the low-density lipoprotein (LDL) and high-density lipoprotein (HDL) fractions in *LeXis*-expressing mice (Fig. 2c). The effects of *LeXis* were distinct from the consequences of hepatic expression of other LXR target genes, such as *Abca1* and *Idol* (also known as *Mylip*), which raise serum cholesterol^{8,9}.

Unbiased pathway analysis of global gene expression revealed that the cholesterol biosynthetic pathway was strongly downregulated in *LeXis*-transduced livers (Extended Data Fig. 4d). These results were validated by qPCR (Fig. 2d). These results suggested that the cholesterol lowering effects of *LeXis* were due, at least in part, to suppression

¹Department of Pathology and Laboratory Medicine, Howard Hughes Medical Institute, University of California, Los Angeles, California 90095, USA. ²Department of Medicine, Division of Cardiology, University of California, Los Angeles, California 90095, USA. ³Department of Human Genetics, University of California, Los Angeles, California 90095, USA. ⁴Ionis Pharmaceuticals, Carlsbad, California 92008, USA. ⁵Pasarow Mass Spectrometry Laboratory, NPI-Semel Institute, University of California, Los Angeles, California 90095, USA.

*These authors contribute equally to this work.

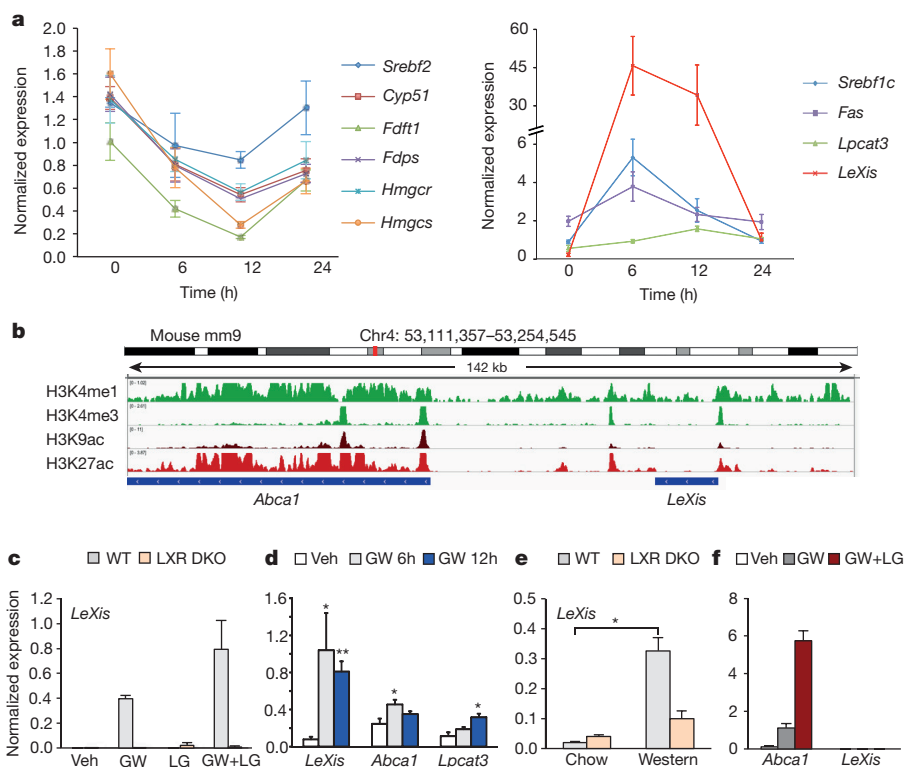


Figure 1 | LXR activation inhibits cholesterol biosynthesis and induces *LeXis* expression. **a**, qPCR analysis of gene expression in livers from C57BL/6 mice treated by oral gavage with 40 mg kg⁻¹ GW3965 for the indicated time ($n = 6$ mice per group). All curves are statistically different from baseline expression ($P < 0.05$, one way analysis of variance (ANOVA)). **b**, Schematic representation of the *LeXis* gene locus on an Integrative Genome Viewer (IGV) showing histone marks from LICR ENCODE data. **c**, qPCR analysis of gene expression in primary mouse hepatocytes treated with GW3965 (GW; 1 μ M) and/or the RXR ligand LG268 (LG; 50 nM). DKO, double knockout (*LXR α* ^{-/-} and *LXR β* ^{-/-}).

Results are representative of four independent experiments. **d**, qPCR analysis of gene expression in livers from male C57BL/6 mice gavaged with 40 mg kg⁻¹ GW3965 before collection at the indicated time ($n = 6$ per group). **e**, Gene expression in livers obtained from mice maintained on chow ($n = 2$ per group) or a Western diet ($n = 5$ per group). **f**, Gene expression in primary mouse peritoneal macrophages treated with 1 μ M GW3965 and/or 50 nM LG268 for 16 h. Results are representative of four independent experiments. Values are mean \pm s.d. (**c**, **f**), or mean \pm s.e.m. (**a**, **d**, **e**). * $P < 0.05$; ** $P < 0.01$ (analysis of variance (ANOVA) with multi-group comparison in **a**, **d** and **e**).

of cholesterol biosynthesis. Consistent with this interpretation, we observed a strong trend towards lower cholesterol content in the livers of mice overexpressing *LeXis* (Extended Data Fig. 4e). For reasons that are not yet clear, treatment of isolated primary hepatocytes did not reflect the effects of either LXR agonist treatment or *LeXis* expression on genes linked to sterol synthesis (Extended Data Fig. 4f, g).

A reduction in plasma cholesterol suggests an increase in lipoprotein clearance or a decrease in sterol production¹⁰. To assess the contribution of the low-density lipoprotein receptor (LDLR) to the actions of *LeXis*, we transduced *Ldlr*^{-/-} mice with control or *LeXis*-expressing adenovirus. We observed decreases in plasma cholesterol levels and hepatic cholesterol content in response to *LeXis* in *Ldlr*^{-/-} mice, suggesting that the LDLR is not required for *LeXis* effects (Fig. 2e and Extended Data Fig. 4h, i). To assess the contribution of SREBP-2 signalling to LXR-mediated inhibition of cholesterologenesis, we administered GW3965 to control or liver-specific SCAP (L-SCAP) knockout mice¹¹. Consistent with previous studies¹², GW3965 treatment did not alter serum cholesterol levels in control mice (Fig. 2f). Notably, however, GW3965 increased serum cholesterol levels in L-SCAP knockout mice, suggesting the loss of a suppressive effect (Fig. 2f, g). LXR target genes, including *LeXis* itself, were induced by GW3965 in both groups; however, the suppression of steroidogenic genes was abrogated in L-SCAP knockout mice (Extended Data Fig. 4j). Furthermore, expression of *LeXis* also failed to lower serum cholesterol or suppress cholesterologenic gene expression in L-SCAP knockout mice (Fig. 2h and Extended Data Fig. 4k).

To address the role of *LeXis* in the setting of dietary cholesterol challenge, we used adenoviral vectors to express short hairpin RNA

(shRNA) constructs targeting *LeXis* in mouse liver^{13,14}. Knockdown of *LeXis* with either of two different shRNA constructs increased serum HDL cholesterol levels in mice fed a Western diet (Extended Data Fig. 5a–d). There was also an increase in liver cholesterol content in sh*LeXis*-transduced mice (Extended Data Fig. 5e). Gene expression analysis revealed increased expression of cholesterol biosynthetic genes in response to *LeXis* knockdown (Extended Data Fig. 5f). Similar effects of *LeXis* knockdown were observed in mice treated with GW3965 (Extended Data Fig. 5g, h). There was no consistent evidence of ER stress or inflammation in these experiments (Extended Data Fig. 5i–k).

As a complementary acute loss-of-function approach, we used anti-sense oligonucleotides (ASOs) to target *LeXis* expression^{15,16}. Three different ASOs that potentially blocked hepatic *LeXis*, but not saline or non-targeting ASO controls, increased serum cholesterol levels in the setting of LXR activation, with no evidence of hepatotoxicity (Fig. 3a, b and Extended Data Fig. 5l, m). Furthermore, *LeXis* ASO administration increased cholesterologenic gene expression (Fig. 3c).

We generated *LeXis*-deficient mice to determine the consequences of chronic loss of *LeXis* function (Extended Data Fig. 6a–c). Although serum cholesterol levels in *LeXis*-deficient mice in the setting of LXR activation were not different from controls (Fig. 3d), the expression of sterol synthesis genes in the liver was increased (Fig. 3e). Furthermore, *LeXis*-null mice had increased hepatic cholesterol content when challenged with a Western diet (Fig. 3f). Gross and histological examination of livers from *LeXis*-deficient null mice showed changes consistent with lipid accumulation (Fig. 3g, h). In contrast to the acute LXR agonist studies above, gene expression analysis of *LeXis*^{-/-} mice maintained

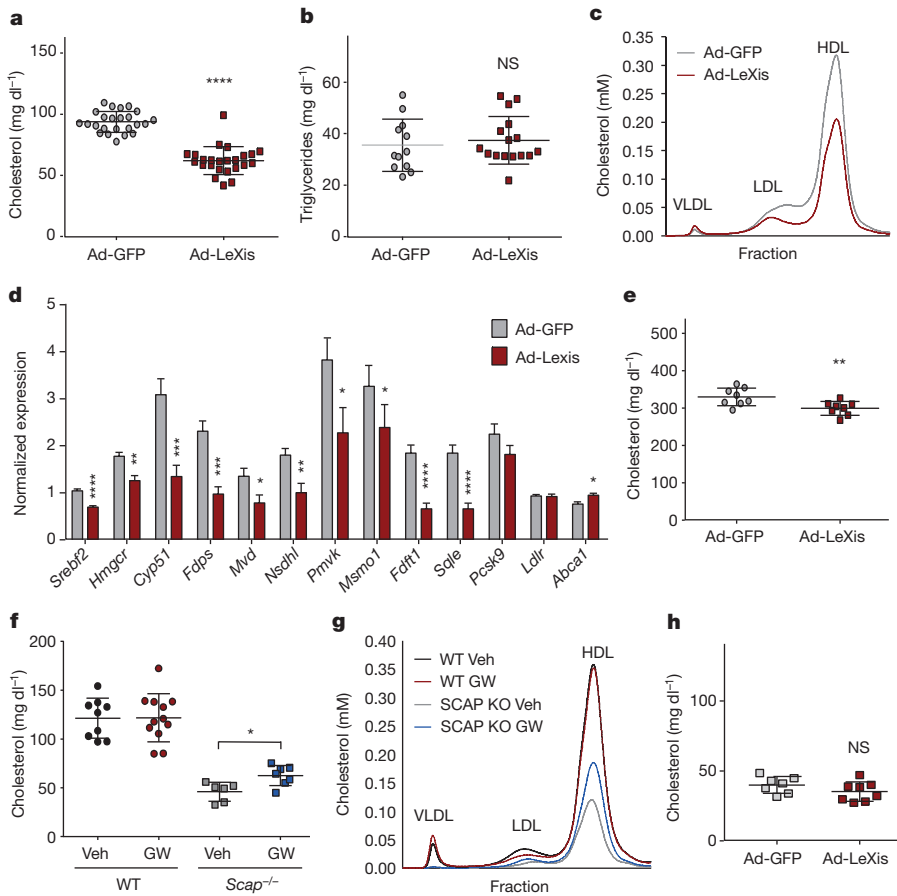


Figure 2 | *LeXis* expression reduces serum cholesterol and sterol synthesis through a pathway requiring intact SREBP signalling. **a**, Total serum cholesterol levels in 10-week-old chow-fed male C57BL/6 mice transduced with adenoviral vectors encoding GFP control (Ad-GFP) or *LeXis* (Ad-*LeXis*) for 6 days ($n = 24$ per group). **b**, Total serum triglycerides levels in the mice shown in **a** ($n = 12-16$ per group). **c**, Cholesterol levels in pooled fractionated serum from mice treated with Ad-GFP or Ad-*LeXis*. VLDL, very-low-density lipoprotein. **d**, Analysis of gene expression in livers obtained after 6 days of transduction with Ad-GFP or Ad-*LeXis* ($n = 8$ per group). **e**, Total serum cholesterol levels in chow-fed male *Ldlr*^{-/-} mice (10 weeks old) transduced with Ad-GFP or Ad-*LeXis* for 6 days ($n = 8$ per group). **f**, Serum cholesterol levels in chow-fed wild-type (WT) or liver-specific SCAP knockout (*Scap*^{-/-}) mice gavaged with 40 mg kg⁻¹ GW3965 for 2 days. **g**, Cholesterol levels in pooled plasma fractions from mice shown in **f**. **h**, Total serum cholesterol levels in chow-fed *Scap*^{-/-} mice transduced with Ad-GFP or Ad-*LeXis* for 6 days. All values are mean \pm s.e.m. NS, not significant; * $P < 0.05$; ** $P < 0.01$; *** $P < 0.001$; **** $P < 0.0001$ (unpaired two-tailed *t*-test).

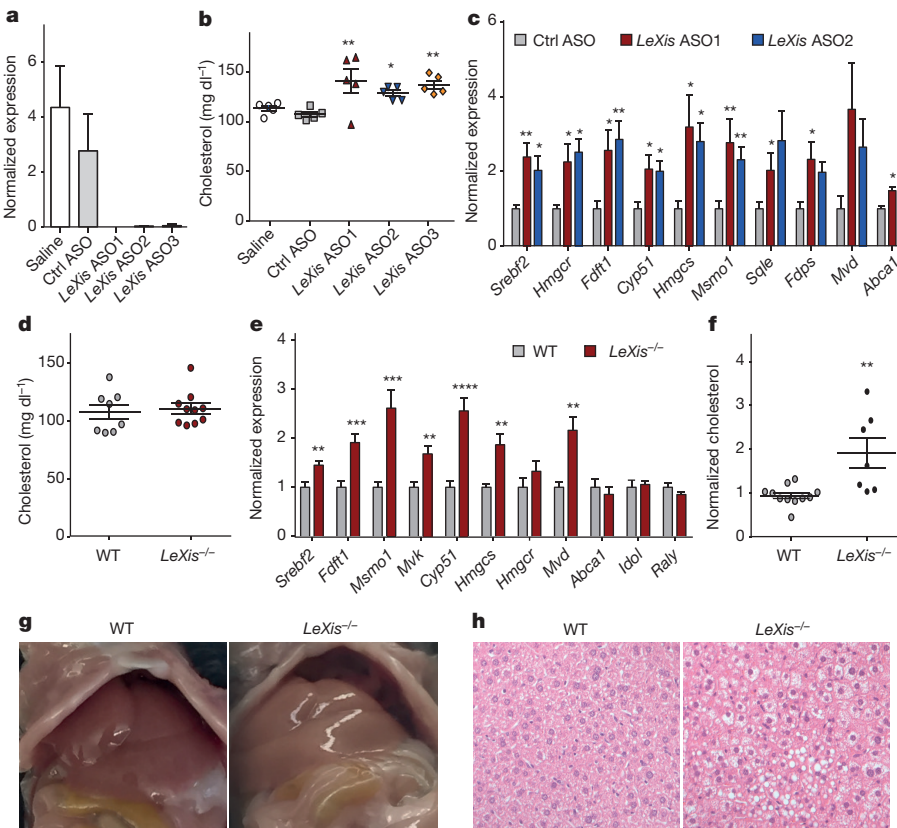


Figure 3 | Acute and chronic inactivation of *LeXis* alters hepatic lipid metabolism. **a**, *LeXis* gene expression (normalized to *36B4*, also known as *Rplp0*) in livers from C57BL/6 mice on a chow diet administered 25 mg kg⁻¹ ASOs intraperitoneally on days 1, 4 and 7, and gavaged with 40 mg kg⁻¹ GW3965 on days 4, 7 and 8 ($n = 5$ per group). Ctrl, control. **b**, Total serum cholesterol from mice in **a**. **c**, Gene expression from C57BL/6 mice on a chow diet administered 25 mg kg⁻¹ ASOs intraperitoneally on days 1, 3 and 5, and gavaged with 40 mg kg⁻¹ GW3965 on days 5 and 6 ($n = 8$ per group). **d**, Total serum cholesterol levels in chow-fed wild-type or *LeXis*^{-/-} mice gavaged with 40 mg kg⁻¹ GW3965 for 2 days ($n = 8-10$ per group). **e**, Gene expression from C57BL/6 wild-type or *LeXis*^{-/-} mice on a chow diet gavaged with 40 mg kg⁻¹ GW3965 for 2 days ($n = 8-10$ per group). **f**, Hepatic cholesterol content was normalized to liver mass from C57BL/6 wild-type or *LeXis*^{-/-} mice fed a Western diet for 3 weeks ($n = 7-11$ per group). **g**, Representative (of three images per group) gross appearance of livers from wild-type and *LeXis*^{-/-} mice after 3 weeks on a Western diet. **h**, Histological sections of liver from wild-type and *LeXis*^{-/-} mice after 3 weeks on a Western diet (haematoxylin and eosin stain representative of three images per group). Original magnifications, $\times 40$ (**g**) and $\times 1$ (**h**). All values (**a-f**) are mean \pm s.e.m. * $P < 0.05$; ** $P < 0.01$; *** $P < 0.001$; **** $P < 0.0001$ (ANOVA (**b**, **c**) and unpaired two-tailed *t*-test (**e**, **f**)).

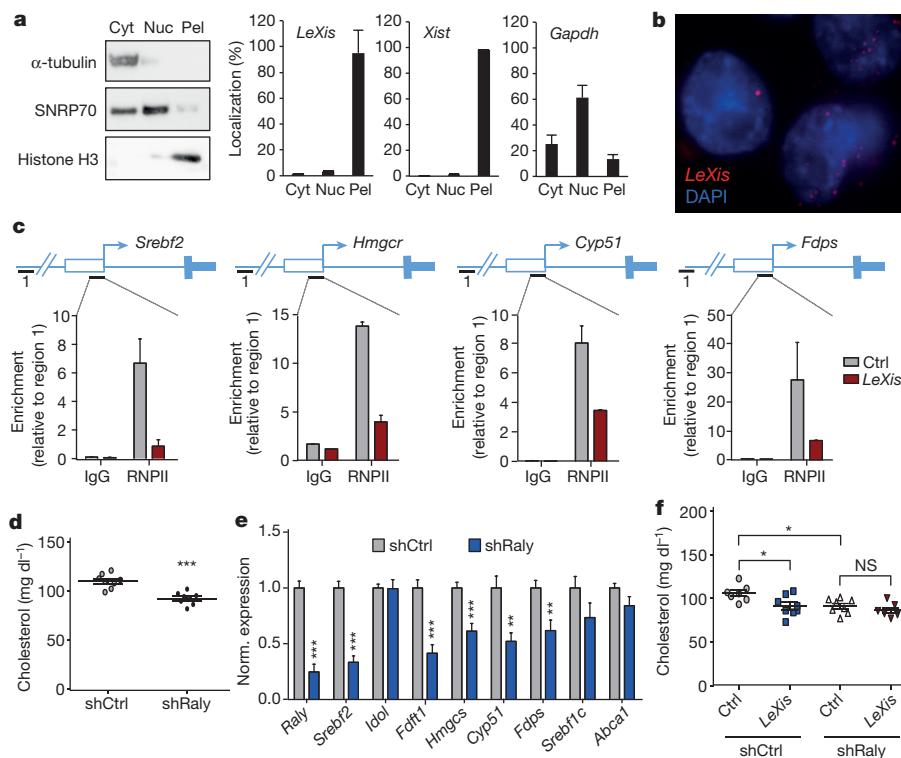


Figure 4 | *LeXis* interacts with RALY to regulate metabolic gene expression. **a**, Hepa1-6 cells were transfected with *LeXis*, and 24 h later cellular content was separated into cytoplasmic soluble (cyt), nuclear soluble (nuc) and insoluble pellet (pel) fractions. Transcripts in each fraction were analysed by qPCR, and fraction purity was validated by western blotting with the indicated compartment markers ($n = 3$ per group). **b**, Representative (of three) micrograph showing *LeXis* subcellular localization in primary mouse hepatocytes by single molecule fluorescence *in situ* hybridization using anti-sense probes to *LeXis* (red). Nuclei were counterstained with DAPI (blue). Original magnification, $\times 63$. **c**, Recruitment of RNA polymerase II (RNPII) to promoter regions as determined by ChIP-qPCR analysis in livers transduced with control

(Ad-GFP) or *LeXis*-expressing (Ad-*LeXis*) adenoviruses. Data are expressed as percentage input retrieved normalized to an upstream site (region 1) ($n = 3$ per group). **d**, Total serum cholesterol levels in 14-week-old chow-fed male C57BL/6 mice transduced with control (shCtrl) or adenoviral vectors expressing *Raly* shRNA (shRaly) ($n = 8$ per group). **e**, Gene expression in livers of the mice shown in **f**. **f**, Total serum cholesterol in chow-fed male C57BL/6 mice transduced with control (Ad-GFP) or Ad-*LeXis* (1.0×10^9 plaque-forming units, p.f.u.) and shCtrl or shRaly (2.0×10^9 p.f.u.) ($n = 7-8$ per group). Values are mean \pm s.d. (**a, c**) or mean \pm s.e.m. (**d, e**). * $P < 0.05$; ** $P < 0.01$; *** $P < 0.001$ (unpaired two-tailed *t*-test (**d, e**) and ANOVA with multi-group comparison (**f**)).

on Western diet showed a trend towards decreased sterol synthetic gene expression, probably reflecting the marked increased hepatic cholesterol content in this setting (Extended Data Fig. 6d).

To begin to understand how *LeXis* was influencing hepatic metabolism, we analysed its subcellular localization. *LeXis* was almost exclusively located in the insoluble nuclear pellet in fractionation studies, along with the known nuclear long non-coding RNAs (lncRNAs) *XIST* and histone H3 (Fig. 4a). Single molecule RNA fluorescence *in-situ* hybridization with *LeXis*-specific probes further confirmed its nuclear localization (Fig. 4b).

Owing to the presence of *LeXis* in the nucleus, we tested its ability to affect RNA polymerase II-dependent transcription. Expression of *LeXis* in mouse liver reduced RNA polymerase II engagement at the promoters of *Srebf2* and its target genes (Fig. 4c). Previous work has shown that nuclear lncRNAs can affect transcription by modifying the recruitment of proteins to chromatin¹⁷. We used an unbiased lncRNA-chromatin affinity capture technique to pull-down *LeXis* from mouse liver and identify interacting proteins¹⁸ (Extended Data Fig. 7a). Analysis of the *LeXis* interactome by mass spectrometry identified the heterogeneous ribonucleoprotein RALY¹⁹ as a binding partner. Similar to *LeXis*, RALY was located in the nuclear pellet (chromatin) fraction of hepatocytes (Extended Data Fig. 7b). Moreover, an antibody to RALY retrieved *LeXis* in co-immunoprecipitation studies (Extended Data Fig. 7c, d).

RALY contains both an RNA-binding domain and a leucine-zipper coiled domain, suggesting it may act as a regulatory factor²⁰.

Notably, previous unbiased analysis of gene coexpression networks has identified *Srebf2* as one of the top genes positively coregulated with *Raly*²¹. Other studies have shown direct binding of SREBP-2 at the *Raly* promoter²². Unbiased protein homology analysis revealed extensive structural conservation between RALY and RNA binding motif protein 14 (RBM14, also known as CoAA)²³ (Extended Data Fig. 7e), a known steroid receptor coactivator²⁴. This led us to hypothesize that RALY may act as transcriptional cofactor for genes involved in cholesterol biosynthesis. In line with this idea, adenovirus-mediated knockdown of RALY in mouse liver reduced serum cholesterol, mimicking the effect of *LeXis* expression (Fig. 4d and Extended Data Fig. 7f). This effect was correlated with reduced expression of *Srebf2* and its target genes (Fig. 4e and Extended Data Fig. 7g). Unbiased gene expression profiling of liver revealed that RALY knockdown preferentially affected cholesterol biosynthetic pathways (Extended Data Fig. 8a, b). The effects of RALY were independent of LDLR expression, since they were preserved in *Ldlr*-null mice (Extended Data Fig. 9a, b). The actions of *LeXis* *in vivo* were dependent on RALY, since the ability of *LeXis* to alter serum cholesterol levels and hepatic gene expression was impaired in the setting of RALY knockdown (Fig. 4f and Extended Data Fig. 9c). Finally, ChIP-qPCR analysis of mouse liver revealed that RALY associated with cholesterol biosynthetic gene promoters, and that RALY occupancy was reduced in the setting of *LeXis* expression (Extended Data Fig. 9d).

This work identifies the non-coding RNA *LeXis* as an additional mediator of the complex effects of LXR signalling on hepatic lipid

metabolism. Our data suggest that *LeXis* contributes to the ability of LXRs to inhibit cholesterol synthesis. It is important to acknowledge, however, that the involvement of additional pathways in this crosstalk is not excluded by the present work. The demonstration that *LeXis* expression is responsive to dietary cues and can modulate physiological pathways with links to common diseases expands our understanding of the regulatory potential of non-coding RNA. Notably, the consequences of acute and chronic loss of *LeXis* expression are only partially overlapping, perhaps reflecting compensation in the setting of developmental deletion²⁵.

Although the rapid sequence evolution of lncRNAs presents a challenge to identifying functional counterparts between species²⁶, batch coordinate conversion between mouse and human assemblies revealed moderate conservation of the *LeXis* genomic sequence in a region adjacent to the human *ABCA1* gene. An annotated putative lncRNA (TCONS_00016452) in this region was robustly induced by LXR activation in human hepatocyte cell lines (Extended Data Fig. 10). In the future it will be of interest to assess whether this sequence or an as yet to be identified lncRNA is a functional orthologue of *LeXis*.

Online Content Methods, along with any additional Extended Data display items and Source Data, are available in the online version of the paper; references unique to these sections appear only in the online paper.

Received 3 August 2015; accepted 18 March 2016.

Published online 11 May 2016.

- Tontonoz, P. Transcriptional and posttranscriptional control of cholesterol homeostasis by liver X receptors. *Cold Spring Harb. Symp. Quant. Biol.* **76**, 129–137 (2011).
- Repa, J. J. *et al.* Regulation of mouse sterol regulatory element-binding protein-1c gene (SREBP-1c) by oxysterol receptors, LXR α and LXR β . *Genes Dev.* **14**, 2819–2830 (2000).
- Zelcer, N., Hong, C., Boyadjian, R. & Tontonoz, P. LXR regulates cholesterol uptake through Idol-dependent ubiquitination of the LDL receptor. *Science* **325**, 100–104 (2009).
- Brown, M. S. & Goldstein, J. L. The SREBP pathway: regulation of cholesterol metabolism by proteolysis of a membrane-bound transcription factor. *Cell* **89**, 331–340 (1997).
- Zhang, Y. *et al.* Liver LXR α expression is crucial for whole body cholesterol homeostasis and reverse cholesterol transport in mice. *J. Clin. Invest.* **122**, 1688–1699 (2012).
- Creyghton, M. P. *et al.* Histone H3K27ac separates active from poised enhancers and predicts developmental state. *Proc. Natl Acad. Sci. USA* **107**, 21931–21936 (2010).
- The ENCODE Project Consortium. An integrated encyclopedia of DNA elements in the human genome. *Nature* **489**, 57–74 (2012).
- Zelcer, N. & Tontonoz, P. Liver X receptors as integrators of metabolic and inflammatory signaling. *J. Clin. Invest.* **116**, 607–614 (2006).
- Vaisman, B. L. *et al.* ABCA1 overexpression leads to hyperalphalipoproteinemia and increased biliary cholesterol excretion in transgenic mice. *J. Clin. Invest.* **108**, 303–309 (2001).
- Horton, J. D., Goldstein, J. L. & Brown, M. S. SREBPs: activators of the complete program of cholesterol and fatty acid synthesis in the liver. *J. Clin. Invest.* **109**, 1125–1131 (2002).
- Matsuda, M. *et al.* SREBP cleavage-activating protein (SCAP) is required for increased lipid synthesis in liver induced by cholesterol deprivation and insulin elevation. *Genes Dev.* **15**, 1206–1216 (2001).
- Hong, C. *et al.* The LXR-Idol axis differentially regulates plasma LDL levels in primates and mice. *Cell Metab.* **20**, 910–918 (2014).
- Carpenter, S. *et al.* A long noncoding RNA mediates both activation and repression of immune response genes. *Science* **341**, 789–792 (2013).
- Yang, F., Zhang, H., Mei, Y. & Wu, M. Reciprocal regulation of HIF-1 α and lincRNA-p21 modulates the Warburg effect. *Mol. Cell* **53**, 88–100 (2014).
- Raal, F. J. *et al.* Mipomersen, an apolipoprotein B synthesis inhibitor, for lowering of LDL cholesterol concentrations in patients with homozygous familial hypercholesterolaemia: a randomised, double-blind, placebo-controlled trial. *Lancet* **375**, 998–1006 (2010).
- Gaudet, D. *et al.* Targeting APOC3 in the familial chylomicronemia syndrome. *N. Engl. J. Med.* **371**, 2200–2206 (2014).
- Rinn, J. L. & Chang, H. Y. Genome regulation by long noncoding RNAs. *Annu. Rev. Biochem.* **81**, 145–166 (2012).
- Chu, C., Quinn, J. & Chang, H. Y. Chromatin isolation by RNA purification (ChIRP). *J. Vis. Exp.* **61**, 3912 (2012).
- Michaud, E. J., Bultman, S. J., Stubbs, L. J. & Woychik, R. P. The embryonic lethality of homozygous lethal yellow mice (*A^yA^y*) is associated with the disruption of a novel RNA-binding protein. *Genes Dev.* **7**, 1203–1213 (1993).
- Jiang, W., Guo, X. & Bhavanandan, V. P. Four distinct regions in the auxiliary domain of heterogeneous nuclear ribonucleoprotein C-related proteins. *Biochim. Biophys. Acta* **1399**, 229–233 (1998).
- Okamura, Y. *et al.* COXPRESdb in 2015: coexpression database for animal species by DNA-microarray and RNAseq-based expression data with multiple quality assessment systems. *Nucleic Acids Res.* **43**, D82–D86 (2015).
- Seo, Y. K. *et al.* Genome-wide localization of SREBP-2 in hepatic chromatin predicts a role in autophagy. *Cell Metab.* **13**, 367–375 (2011).
- Kelley, L. A., Mezulis, S., Yates, C. M., Wass, M. N. & Sternberg, M. J. The Phyre2 web portal for protein modeling, prediction and analysis. *Nature Protocols* **10**, 845–858 (2015).
- Auboeuf, D. *et al.* CoAA, a nuclear receptor coactivator protein at the interface of transcriptional coactivation and RNA splicing. *Mol. Cell. Biol.* **24**, 442–453 (2004).
- Rossi, A. *et al.* Genetic compensation induced by deleterious mutations but not gene knockdowns. *Nature* **524**, 230–233 (2015).
- Ulitsky, I., Shkumatava, A., Jan, C. H., Sive, H. & Bartel, D. P. Conserved function of lincRNAs in vertebrate embryonic development despite rapid sequence evolution. *Cell* **147**, 1537–1550 (2011).

Supplementary Information is available in the online version of the paper.

Acknowledgements We thank members of the Tontonoz, Nagy, Smale and Black laboratories and the UCLA Atherosclerosis Research Unit for technical assistance and useful discussions. This work was supported by NIH grants HL030568, HL066088, DK063491, HL128822, DK102559 and HL69766; American Heart Association grant 13POST17080115; American College of Cardiology Presidential CDA; and the UCLA Cardiovascular Discovery Fund (Lauren B. Leichtman and Arthur E. Levine Investigator Award).

Author Contributions T.S. and P.T. conceived and designed the study, guided the interpretation of the results and the preparation of the manuscript. P.T. supervised the study and provided critical suggestions. T.S. and X.W. performed most mouse experiments and data analysis. M.C.J., T.G., L.Z., J.S., C.H., T.d.A.V. participated in mouse experiments and data analysis. T.S. performed RNA-seq experiments and validated *LeXis* as an LXR target. A.E. and D.C. processed and analysed next-generation sequencing data. M.C.J. performed and analysed the RACE experiments. J.W. performed the mass spectrometry analysis. M.K. and R.L. provided and independently validated ASOs targeting *LeXis*. T.S. and P.T. drafted the manuscript. T.S., M.C.J. and P.T. edited the manuscript with input from all authors. All authors discussed the results and approved the final version of the manuscript.

Author Information Sequencing and microarray data have been deposited in the Gene Expression Omnibus (GEO) under accessions GSE77793, GSE77786, GSE77802 and GSE77805. Reprints and permissions information is available at www.nature.com/reprints. The authors declare no competing financial interests. Readers are welcome to comment on the online version of the paper. Correspondence and requests for materials should be addressed to P.T. (ptontonoz@mednet.ucla.edu).

METHODS

Reagents, plasmids and gene expression. GW3965 was synthesized as previously described²⁷. LG268 was from Ligand Pharmaceuticals. Oxysterols were purchased from Sigma and used as described²⁸. Simvastatin sodium salt was from Calbiochem. Ligands were dissolved in dimethyl sulfoxide before use in cell culture. *LeXis* was amplified from GW3695-treated primary mouse hepatocytes using KOD polymerase (Millipore) and primers designed to provide flanking attB sequences and a SacI site at the immediate 3' end. The fragments were then cloned into pDONR221 using the Gateway system and the minimal SV40 polyadenylation sequence was inserted at the SacI site. For transient transfections and viral vector production the entry clone was transferred into the pAd/CMV/V5-DEST Gateway vector by LR recombination. We estimate transcription from this vector to append 109 nucleotides at the 5' end, and 29 nucleotides at the 3' end of the cloned *LeXis* sequence. To obtain the sh*LeXis* adenovirus, we used BLOCK-iT kit as described (Invitrogen)³. In brief, Invitrogen based software was used for original nucleotide generation targeting the LEXIS fragment and cloned into pENTR/U6. The resulting pENTR/U6-LEXIS shRNA plasmids were tested for their ability to inhibit overexpressed LEXIS in transient transfection experiments in HEK293T cells and then transferred by Gateway recombination into the pAd/BLOCK-iT-DEST destination vector for viral particle generation. Viruses were amplified, purified and titred by Viraquest. For gene expression analysis, RNA was isolated using TRIzol reagent (Invitrogen) and analysed by qPCR using an Applied Biosystems 7900HT sequence detector or Applied Biosystems Quant Studio 6 Flex. Results are normalized to *36B4* or cyclophilin (also known as *Ppia*). Immunohistochemical staining of paraffin-embedded livers were done by the UCLA Translational Pathology Core Laboratory.

Animals and diets. All animals (C57BL/6, greater than 10 generations backcrossed) were housed in a temperature-controlled room under a 12-h light/12-h dark cycle and pathogen-free conditions. For adenovirus experiments, age-matched mice were purchased from Jackson Laboratories. Littermates were manually randomized to different treatment groups. Investigators were blinded to group allocation for some but not all studies. *LXR α ^{-/-}*, *LXR β ^{-/-}* and *LXR α β ^{-/-}* mice were originally provided by D. Mangelsdorf. Floxed *Scap^{-/-}* mice were previously described²⁹. *LeXis* global knockout mice were generated at UC Davis KOMP using strategy outlined in Extended Data Fig. 6. Mice were fed a chow diet except as indicated, where mice were placed on a Western diet (21% fat, 0.21% cholesterol; D12079B; Research Diets Inc.) or were gavaged with either vehicle or 40 mg kg⁻¹ GW3965. Livers were obtained 4 h after the last gavage. We measured cholesterol and triglycerides as previously described³⁰. For adenoviral infections, age-matched (9–11 weeks old) male mice were injected with 2.0×10^9 p.f.u. by tail-vein injection unless otherwise specified. Mice were euthanized 6 days later after a 6-h fast. At the time of euthanization, liver tissue and blood was collected by cardiac puncture and immediately frozen in liquid nitrogen and stored at -80°C . Liver tissue was processed for isolation of RNA and protein as above. Generation 2.5 constrained ethyl ASOs, synthesized as described previously³¹, were administered by three 25 mg kg⁻¹ intraperitoneal doses together with 40 mg kg⁻¹ GW3965. Animals were euthanized on day 6 or 8 as indicated in figure legends. Most experiments were performed using male mice. All animal experiments were approved by the UCLA Institutional Animal Care and Research Advisory Committee.

Cell culture. Primary peritoneal macrophages were isolated 4 days after thioglycollate injection and prepared as described³². Mouse primary hepatocytes were isolated as previously described and cultured in William's E medium with 5% FBS²⁸. Peritoneal cells were incubated in 0.5% FBS in DMEM, with 5 μM simvastatin and 100 μM mevalonic acid. Five to eight hours later, cells were pretreated with dimethylsulfoxide (DMSO) or appropriate ligand overnight. *In vitro* translation assay was performed using TnT Coupled Transcription/Translation System (PROMEGA) according to the manufacturer's protocol. The cell lines HEK293T, HEK293A and Hepa1-6 were originally obtained from ATCC. All cells were tested for mycoplasma contamination.

RACE. The 5' and 3' ends of the *LeXis* transcript were defined using mouse liver RNA and the FirstChoice RLM-RACE kit (Ambion) according to manufacturer's protocol, with modifications. In brief, for the 5' RACE, degraded messenger RNA 5' ends were dephosphorylated with CIP, and then full-length mRNA was decapped with TAP. Following 5' RACE adaptor ligation, reverse transcription was performed using SuperScriptIII First-Strand Synthesis system (Invitrogen) and *LeXis*-specific primers. For the 3' RACE, RNA was reverse transcribed using SuperScriptIII First-Strand Synthesis system (Invitrogen) and the adaptor-linked oligo dTs. The resulting cDNA was amplified by nested PCR across a 55–65°C melting temperature gradient using KOD polymerase (Millipore), with the inner primers containing attB sequences. Aliquots of reactions were inspected on 1% agarose gels for product size and abundance. Products of select PCR reactions were purified using NucleoSpin Gel and PCR Cleanup kit (Clontech) and were inserted

into pDONR221 by Gateway cloning. Cloned fragments were sequenced and then aligned to the mouse genome with the BLAST analysis tool.

RNA fractionation. The pAd/CMV-*LeXis* vector was transfected into Hepa1-6 cells using BioT reagent (Bioland Scientific LLC) and 24 h later subcellular RNA fractions were obtained according to the protocol described previously³³. Lysate aliquots were inspected for fractional purity by western blotting with antibodies against α -tubulin, SNRP70 and histone H3 as cytoplasmic, nucleoplasmic and chromatin bound markers, respectively.

RNA-seq. RNA-seq libraries, starting with 500 ng total RNA, were constructed with the TruSeq RNA Sample Prep Kits from Illumina on RNA isolated from primary hepatocytes treated with or without GW3965. Samples were indexed with adapters and submitted for paired-end 2 \times 100-bp sequencing in Illumina HiSeq2000. RNA-seq reads were aligned with TopHatv2.0.2 to the mouse genome, version mm9 (ref. 34). The TopHat alignment rate was 85%, resulting in an average of 65 million reads per sample. Transcripts were assessed and quantities were determined by Cufflinks v2.0.2, using a GTF file based on Ensembl mouse NCBI37. Comparison expression levels were made using fragments per kilobase of exon per million fragments mapped (FPKM) values using Cuffdiff from the Cufflinks package³⁵. Data analysis was performed by UCLA DNA Microarray Core.

Lipid analysis. Tissue lipid was obtained using a Folch extraction. In brief, chloroform extracts were dried under nitrogen and solubilized in water. Tissue and serum cholesterol and triglycerides were determined using a commercially available enzymatic kit (Wako). Hepatic cholesterol content was normalized to liver weight and protein concentration. Mice were fasted for at least 6 h before blood collection and euthanization. Plasma lipoprotein fractions were analysed by FPLC.

Microarray. For cDNA microarray analysis, primary hepatocytes cells were treated as indicated above with either DMSO or GW3965. These samples were from an independent cohort from those submitted for RNA-seq. For each condition, two independent samples were processed. Transcriptional profiling was performed at the University of California, Los Angeles, microarray core facility by using Agilent SurePrint G3 Gene Expression array. Data were analysed using GeneSpring software (Agilent Technologies) and David³⁶.

ChIP. ChIP studies were performed as described elsewhere³⁷. In brief, mouse livers were cross-linked using a final formaldehyde concentration of 1% at room temperature for 10 min. The reaction was quenched with the addition of glycine. For sonication, 0.3 ml (1/3) of nuclear lysate was sonicated for 25–30 cycles, 30 s on 30 s off at 4°C, with BioRuptor twin sonicator (Diagenode). Sonicated Chromatin was incubated overnight at 4°C with control IgG or 25 μg of anti-LXR α antibody (PPZ0412, ChIP Ggade, Abcam), anti-RALY antibody (EPRI0121, Abcam), or Pol II antibody (N-20, Santa Cruz Biotechnology). Protein A dynabeads (50 μl per immunoprecipitation sample) were added for 4 h. After incubation beads were washed with wash buffer A (50 mM HEPES, pH 7.9, 140 mM NaCl, 1 mM EDTA, 1% Triton X-100, 0.1% Na-deoxycholate, 0.1% SDS, 1 \times protease inhibitors freshly added), buffer B (50 mM HEPES, pH 7.9, 500 mM NaCl, 1 mM EDTA, 1% Triton X-100, 0.1% Na-deoxycholate, 0.1% SDS) and finally LiCl buffer (20 mM Tris, pH 8.0, 250 mM LiCl, 1 mM EDTA, 0.5% Na-deoxycholate, 0.5% NP-40). Reverse crosslinking was performed at 60°C overnight, mixed at 1,000 r.p.m., and DNA was extracted using a phenol–chloroform phase lock tube (5 PRIME) or Nucleospin PCR cleanup column (Macherey-Nagel). A standard curve for PCR was generated from serial dilutions of input samples and data expressed as percentage of input.

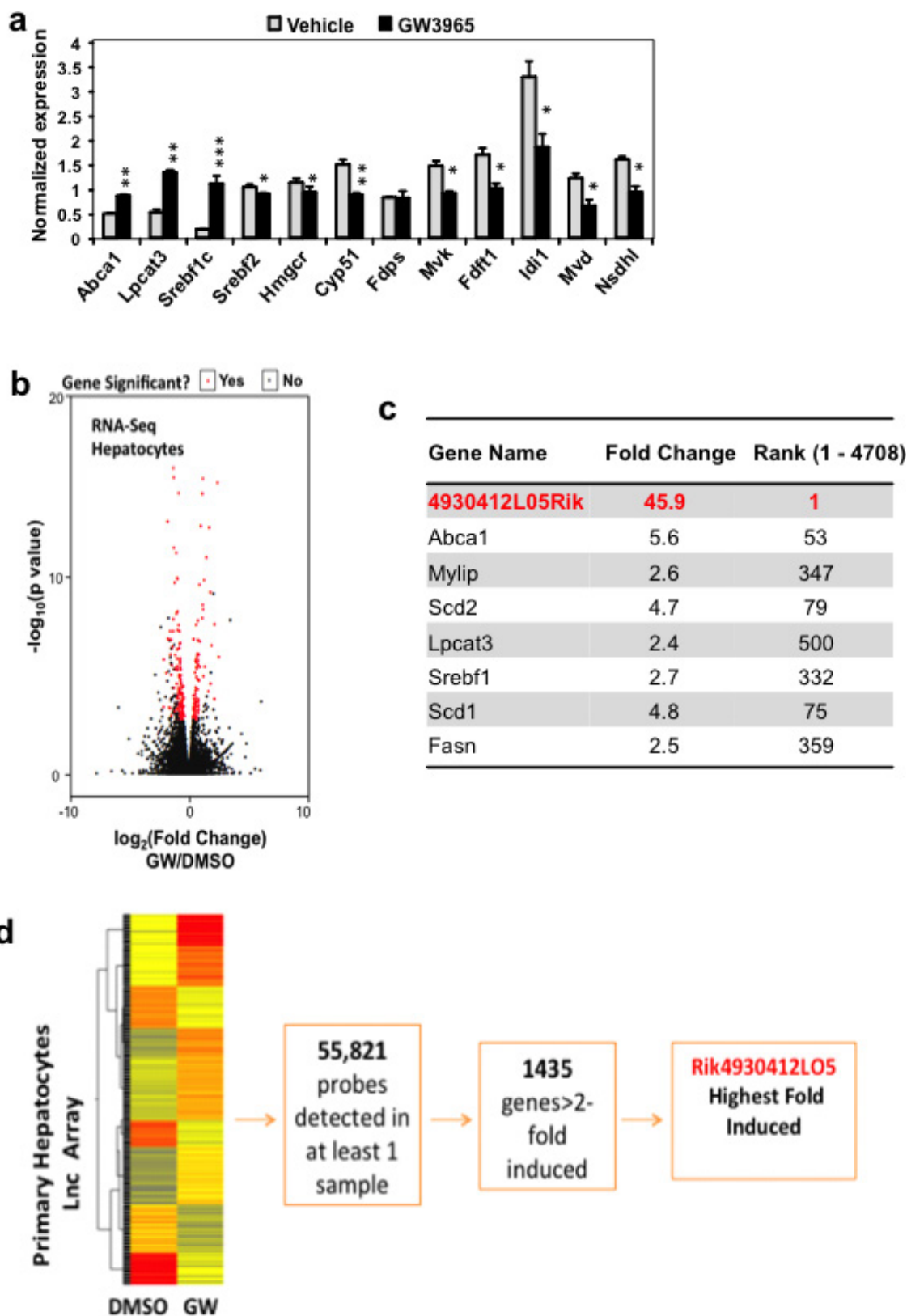
Chromatin isolation by RNA purification. Chromatin isolation by RNA purification (ChIRP) was performed as described previously¹⁸. In brief, mouse livers were cross-linked using glutaraldehyde. After glycine quenching, the nuclear lysate was sonicated for 25–30 cycles, 30 s on 30 s off at 4°C, with BioRuptor twin sonicator (Diagenode). *LeXis* and LacZ pull-down probes with BiotinTEG at 3' were designed by Biosearch Technologies (see Supplementary Information) and allowed to hybridize overnight with sonicated chromatin at 37°C (100 pmol probe per 1 ml chromatin). After hybridization, C1 Dynabeads (Life Technologies) were added and incubated for 30 min. For protein elution for mass spectrometry analysis, washed beads were resuspended in 3 \times original volume of DNase buffer (100 mM NaCl and 0.1% NP-40), and protein was eluted with a cocktail of 50 mM triethyl ammonium bicarbonate, 12 mM sodium lauryl sarcosine, and 0.5% sodium deoxycholate supplemented with 100 $\mu\text{g ml}^{-1}$ RNase A (Sigma-Aldrich) and 0.1 U μl^{-1} RNase H (Epicentre), and 100 U ml^{-1} DNase I (Invitrogen). For RNA isolation, beads were resuspended in proteinase K buffer (100 mM NaCl, 10 mM TrisCl, pH 7.0, 1 mM EDTA, 0.5% SDS, 5% by volume proteinase K (AM2546, Ambion) 20 mg ml⁻¹) and incubated at 50°C followed by Trizol isolation and DNase treatment.

Single molecule RNA FISH. Custom Stellaris FISH probes were designed against *LeXis*. Stellaris probe set labelled with CAL Fluor Red 610 and RNA FISH performed as described previously³⁸. In brief, hepatocytes were fixed with 3.7%

formaldehyde in PBS followed by 70% ethanol treatment to permeabilize cells. Cells were washed with 10% formamide in $2\times$ SSC followed by treatment in humidified chamber with addition of probes (125 nM) in hybridization buffer (100 mg ml^{-1} dextran sulfate and 10% formamide in $2\times$ SSC). Cells were incubated in the dark at 37°C for 4 h. DAPI nuclear stain (5 ng ml^{-1}) was applied after washing with 10% formamide in $2\times$ SSC. Images obtained using a Zeiss Z1 AxioObserver fluorescent microscope.

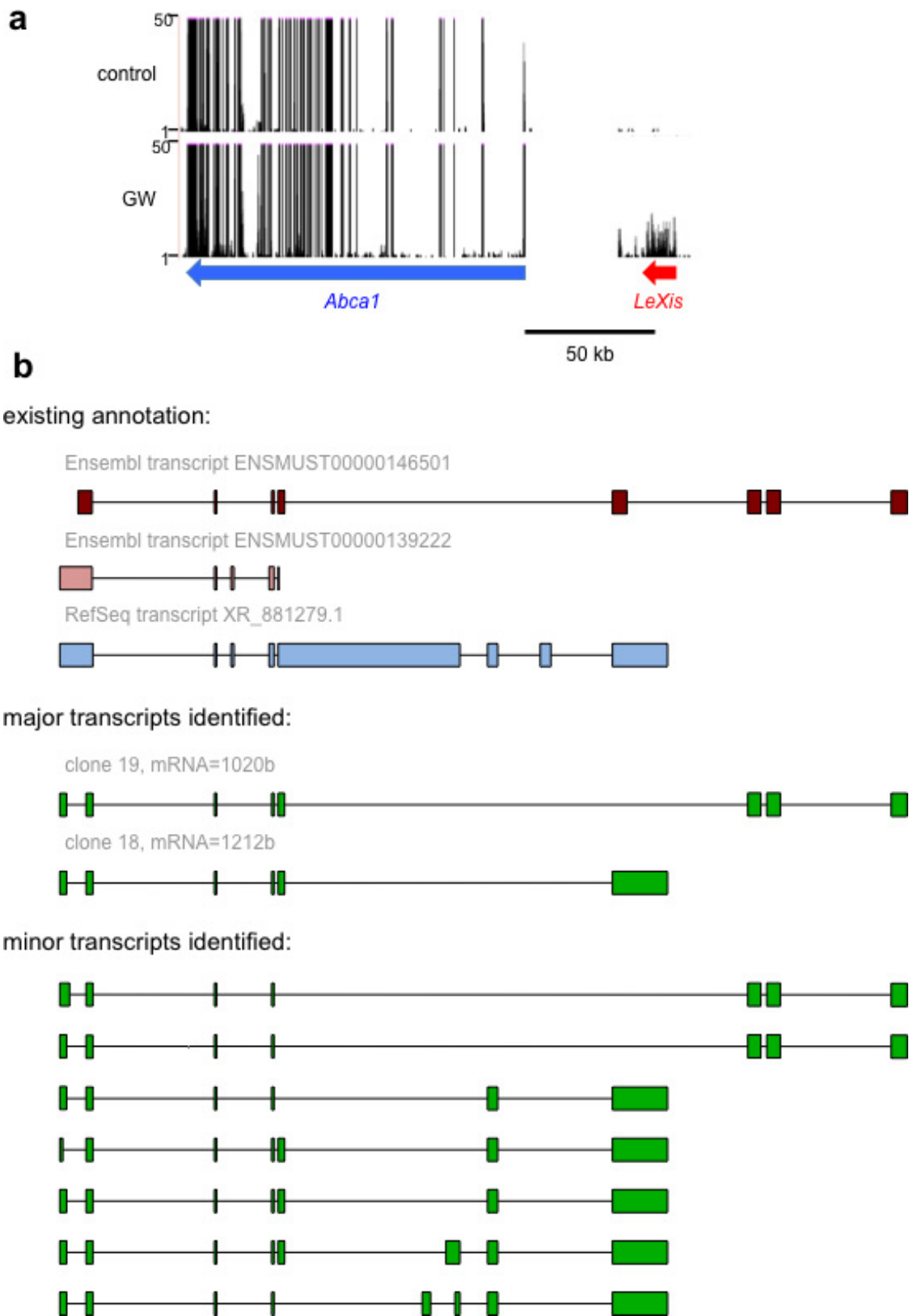
Statistical analysis. A non-paired Student's *t*-test or ANOVA was used to determine statistical significance, defined at $P < 0.05$. Unless otherwise noted, error bars represent s.d.. Experiments were independently performed at least twice. Group sizes were based on statistical analysis of variance and prior experience with similar *in vivo* studies.

27. Sallam, T. *et al.* The macrophage LBP gene is an LXR target that promotes macrophage survival and atherosclerosis. *J. Lipid Res.* **55**, 1120–1130 (2014).
28. Rong, X. *et al.* LXRs regulate ER stress and inflammation through dynamic modulation of membrane phospholipid composition. *Cell Metab.* **18**, 685–697 (2013).
29. Tarling, E. J., Ahn, H. & de Aguiar Vallim, T. Q. The nuclear receptor FXR uncouples the actions of miR-33 from SREBP-2. *Arterioscler. Thromb. Vasc. Biol.* **35**, 787–795 (2015).
30. Hong, C. *et al.* LXR α is uniquely required for maximal reverse cholesterol transport and atheroprotection in ApoE-deficient mice. *J. Lipid Res.* **53**, 1126–1133 (2012).
31. Seth, P. P. *et al.* Short antisense oligonucleotides with novel 2'–4' conformationally restricted nucleoside analogues show improved potency without increased toxicity in animals. *J. Med. Chem.* **52**, 10–13 (2009).
32. Bradley, M. N. *et al.* Ligand activation of LXR β reverses atherosclerosis and cellular cholesterol overload in mice lacking LXR α and apoE. *J. Clin. Invest.* **117**, 2337–2346 (2007).
33. Bhatt, D. M. *et al.* Transcript dynamics of proinflammatory genes revealed by sequence analysis of subcellular RNA fractions. *Cell* **150**, 279–290 (2012).
34. Trapnell, C., Pachter, L. & Salzberg, S. L. TopHat: discovering splice junctions with RNA-Seq. *Bioinformatics* **25**, 1105–1111 (2009).
35. Trapnell, C. *et al.* Transcript assembly and quantification by RNA-Seq reveals unannotated transcripts and isoform switching during cell differentiation. *Nature Biotechnol.* **28**, 511–515 (2010).
36. Huang, D. W., Sherman, B. T. & Lempicki, R. A. Systematic and integrative analysis of large gene lists using DAVID bioinformatics resources. *Nature Protocols* **4**, 44–57 (2009).
37. Carey, M. F., Peterson, C. L. & Smale, S. T. Chromatin immunoprecipitation (ChIP). *Cold Spring Harb. Protoc.* **2009**, pdb.prot5279 (2009).
38. Raj, A. & Tyagi, S. Detection of individual endogenous RNA transcripts in situ using multiple singly labeled probes. *Methods Enzymol.* **472**, 365–386 (2010).



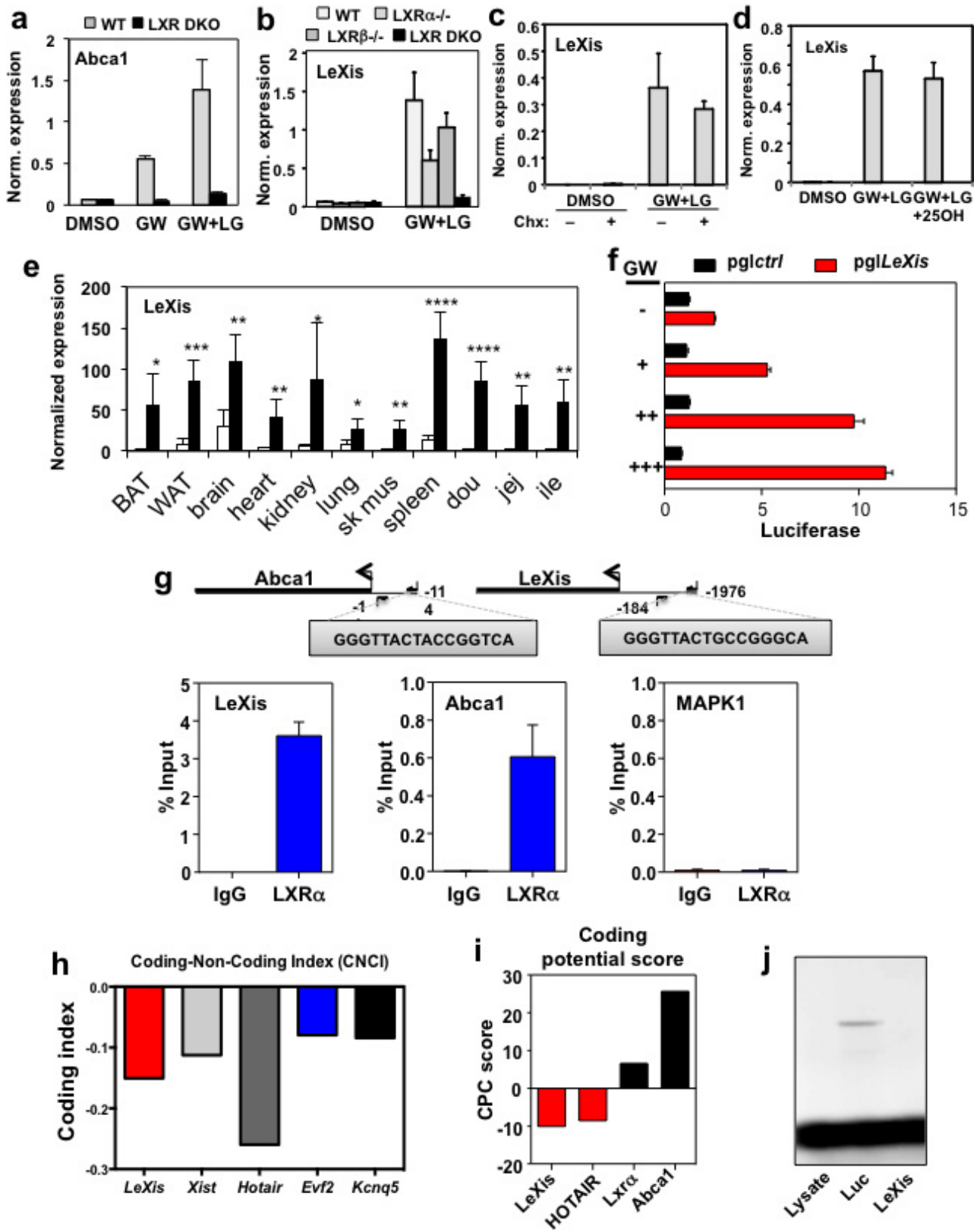
Extended Data Figure 1 | Identification of *LeXis* as an LXR-responsive lncRNA. **a**, qPCR analysis of gene expression in livers from mice gavaged with 40 mg kg^{-1} GW3965 for 2 days. Mice were fasted for 4 h before collection ($n = 4$ per group). Values are mean \pm s.e.m. * $P < 0.05$; ** $P < 0.01$; *** $P < 0.001$ (unpaired two-tailed t -test). **b**, Volcano plot of RNA-seq results from primary hepatocytes treated for 16 h with $1 \mu\text{M}$ GW3965. **c**, Relative expression of selected LXR target genes identified in

the RNA-seq study shown in **b**. Fold change represents ratio of transcript expression in GW3965 compared to DMSO treatment samples. Cut-off fold induction of 1.1 used (total 4,708 transcripts induced). **d**, Heat map representation of the results of transcriptional profiling (Agilent SurePrint G3 Gene Expression arrays) of primary hepatocytes treated with $1 \mu\text{M}$ GW3965 for 16 h. Data were analysed using GeneSpring software.



Extended Data Figure 2 | Schematic of the *LeXis* gene locus and its RNA transcripts. a, UCSC genome browser view of RNA-seq transcriptional signatures at the *Abca1* and *LeXis* locus in mouse primary hepatocytes

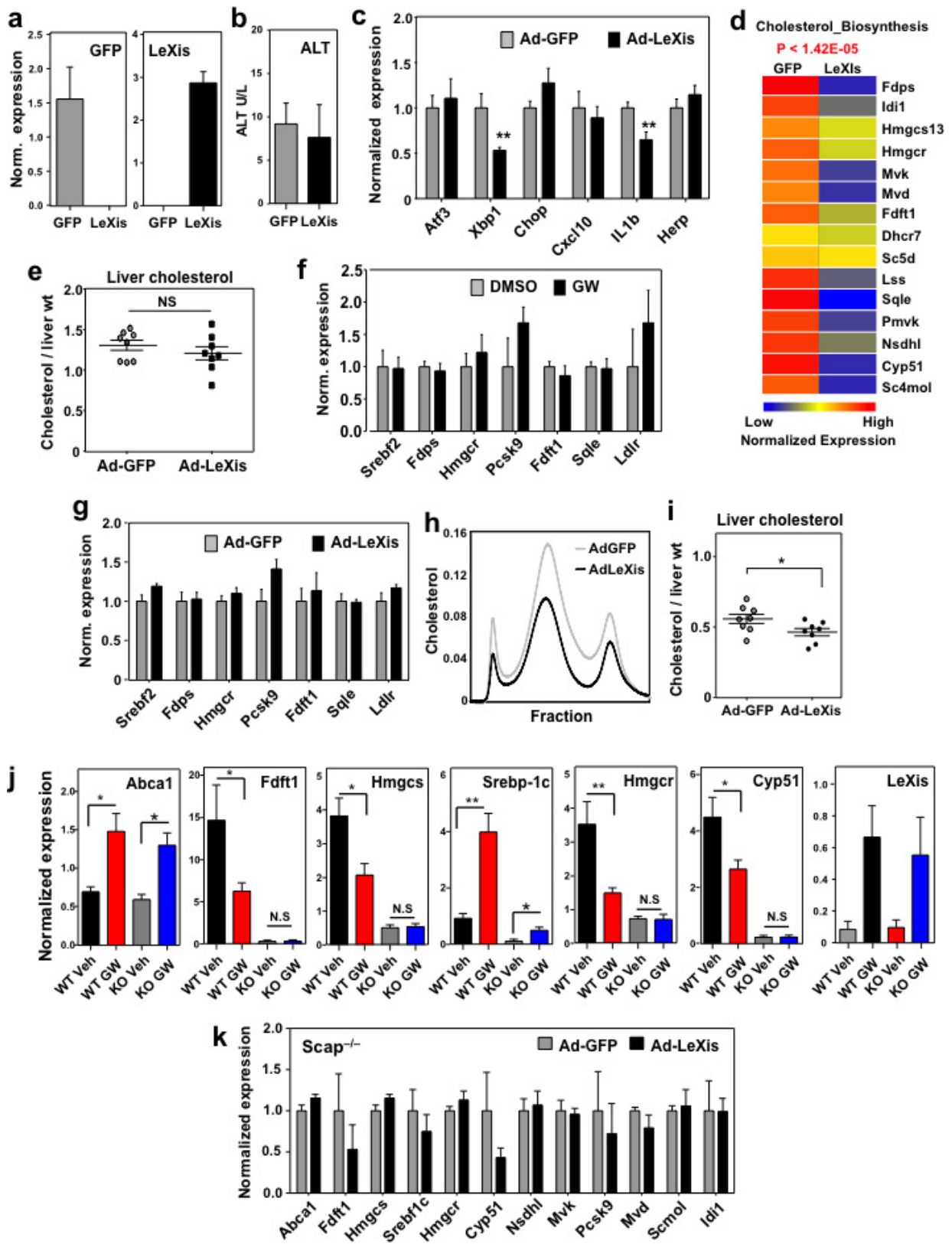
treated with 1 μ M GW3965 for 16 h. **b**, Exon structure of major and minor *LeXis* transcripts identified by RACE, aligned for comparison to existing annotation in the indicated databases.



Extended Data Figure 3 | See next page for caption.

Extended Data Figure 3 | Regulation of *LeXis* expression. **a**, qPCR analysis of primary mouse hepatocytes from wild-type or double knockout (*LXR α* ^{-/-} and *LXR β* ^{-/-}) mice treated with 1 μ M GW3965 and/or 50 nM LG268. Results are representative of four independent experiments. **b**, *LeXis* expression in primary mouse hepatocytes from wild-type, *LXR α* ^{-/-}, *LXR β* ^{-/-} or double knockout mice treated with GW3965 and LG268. Results are representative of three independent experiments. **c**, *LeXis* expression in primary hepatocytes treated with GW3965 and LG268 in the presence or absence of the protein synthesis inhibitor cycloheximide (Chx, 1 μ g μ l⁻¹). Results are representative of three independent experiments. **d**, *LeXis* expression in primary hepatocytes treated with GW3965 and LG268 (50 nM) in the presence or absence of 25-hydroxycholesterol (25OH, 2.5 μ M). Results are representative of three independent experiments. **e**, Gene expression in tissues from C57BL/6 mice gavaged with 40 mg kg⁻¹ GW3965 for 3 days ($n = 5$ per group). * $P < 0.05$; ** $P < 0.01$; *** $P < 0.001$; **** $P < 0.0001$ (unpaired two-tailed

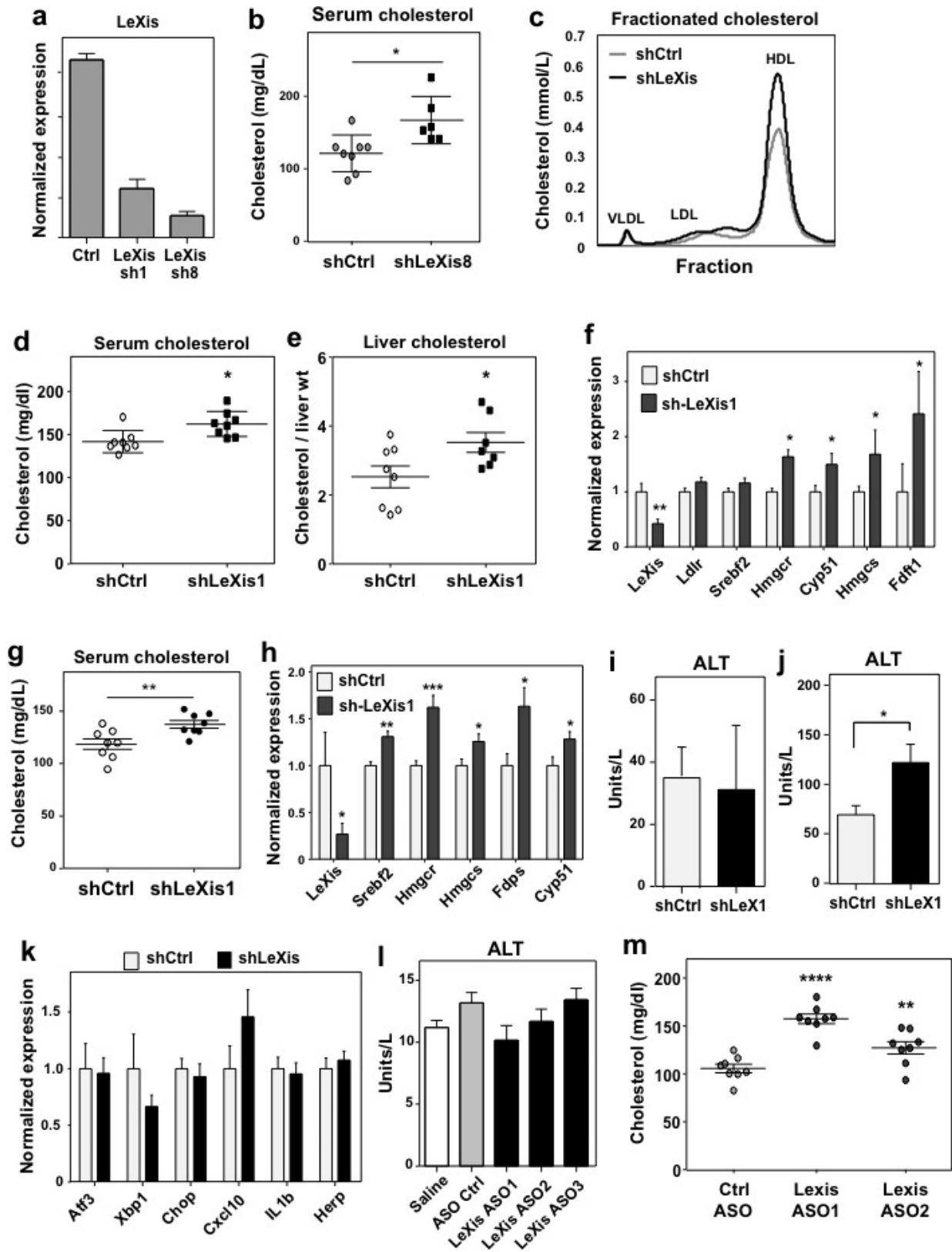
t-test). **f**, Relative firefly luciferase activity measured from the pgl4.10 vector or pgl4.10 with the *LeXis* promoter cloned upstream of luciferase. Reporters were co-transfected in HEK293 cells and treated with GW3965 for 24 h. Activity is normalized to *Renilla* luciferase internal control. **g**, Analysis of LXR α binding to the *LeXis* promoter in mouse liver by ChIP-qPCR. Schematic shows primer pair positions relative to the LXR-response element in the *LeXis* and *Abca1* (positive control) promoters. Primers flanking a region of the MAP kinase I promoter served as a negative control. ChIP values are presented as percentage of input DNA ($n = 4$ per group). Values are mean \pm s.e.m. (**e**, **g**) or mean \pm s.d. (**a-d**). **h**, Prediction of coding potential using the coding-non-coding index (CNCI) software. Negative value indicates low coding potential. **i**, Comparison of protein coding potential using coding potential calculator (CPC) score for *LeXis*, the non-coding gene *HOTAIR*, and control protein-coding transcripts. **j**, *In vitro* translation of *LeXis* and luciferase control RNAs.



Extended Data Figure 4 | See next page for caption.

Extended Data Figure 4 | *LeXis* modulates the expression of genes linked to sterol synthesis. **a**, Gene expression in livers obtained after 6 days of transduction with Ad-GFP or Ad-*LeXis* ($n = 8$ per group). **b**, Serum alanine aminotransferase activity in chow-fed mice transduced with Ad-GFP or Ad-*LeXis* for 6 days ($n = 8$ per group). **c**, Gene expression in livers obtained after 6 days of transduction with Ad-GFP or Ad-*LeXis* ($n = 8$ per group). **d**, Unbiased pathway analysis (GeneSpring software) of the results from transcriptional profiling of livers treated with Ad-GFP or Ad-*LeXis* ($n = 4$ per group). **e**, Hepatic cholesterol content normalized to liver mass in wild-type mice transduced with Ad-GFP or Ad-*LeXis* ($n = 8$ per group). **f**, Gene expression in mouse hepatocytes treated overnight with $1 \mu\text{M}$ GW3965. Results are representative of two independent

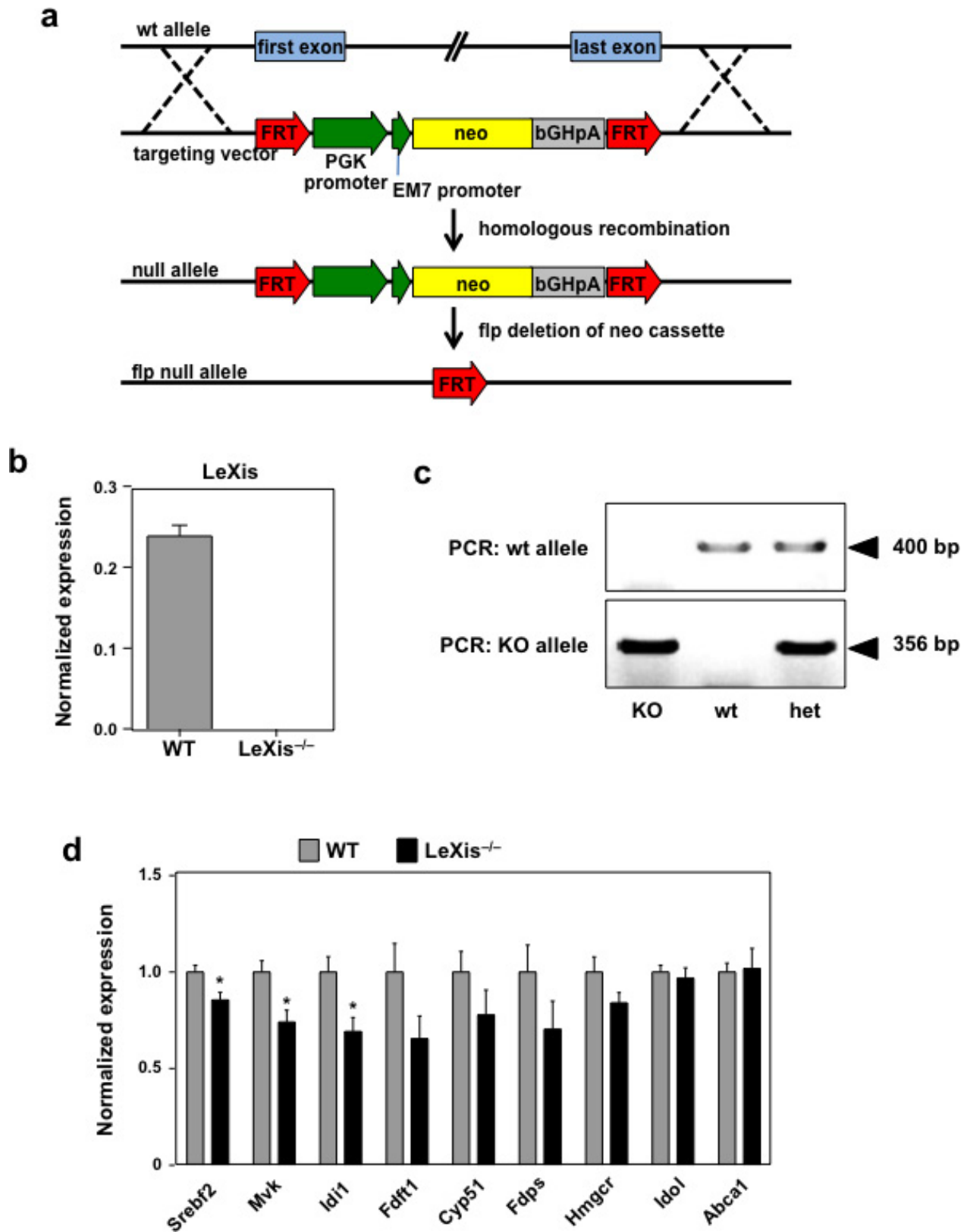
experiments. **g**, Gene expression in mouse hepatocytes treated overnight with Ad-GFP or Ad-*LeXis* for 24 h. Results are representative of two independent experiments. **h**, Cholesterol levels in pooled fractionated serum from *Ldlr*^{-/-} mice transduced with Ad-GFP or Ad-*LeXis*. **i**, Hepatic cholesterol content normalized to liver mass in *Ldlr*^{-/-} mice transduced with Ad-GFP or Ad-*LeXis* ($n = 8$ per group). **j**, Gene expression in livers from chow-fed wild-type or liver-specific *Scap*^{-/-} mice gavaged with 40 mg kg^{-1} GW3965 for 2 days ($n = 5$ (WT Veh), 8 (WT GW), 5 (KO Veh) and 7 (KO GW)). **k**, Gene expression in livers from *Scap*^{-/-} chow-fed mice transduced with Ad-GFP or Ad-*LeXis* for 6 days ($n = 5$ per group). Values are mean \pm s.e.m. (**a–c**, **e**, **i–k**) or mean \pm s.d. (**f**, **g**). * $P < 0.05$; ** $P < 0.01$ (unpaired two-tailed *t*-test).



Extended Data Figure 5 | See next page for caption.

Extended Data Figure 5 | Inhibition of *LeXis* expression alters serum cholesterol level. **a**, *In vitro* validation of *LeXis* knockdown using shLeXis1 and shLeXis8 vectors. Results are representative of three independent experiments. **b**, Total serum cholesterol measured in C57BL/6 mice fed 2 weeks of a Western diet and transduced with adenovirus shCtrl or shLeXis8 for 6 days ($n = 6-8$ per group). **c**, Cholesterol levels in pooled fractionated serum from mice transduced with shCtrl or shLeXis adenovirus. **d**, Total serum cholesterol from male C57BL/6 mice fed a Western diet for 2 weeks and then transduced with control (shCtrl) or adenoviral vectors expressing shRNA targeting *LeXis* (shLeXis1) ($n = 8$ per group). **e**, Hepatic cholesterol content normalized to liver mass for the mice shown in **d** ($n = 8$ (shCtrl) and 7 (shLeXis1)). **f**, Gene expression in livers of mice fed a Western diet for 2 weeks and then transduced with shCtrl or shLeXis ($n = 8$ (shCtrl) and 7 (shLeXis1)). **g**, Total plasma cholesterol levels in chow-fed C57BL/6 mice transduced with shCtrl or shLeXis adenovirus and gavaged with 40 mg kg^{-1}

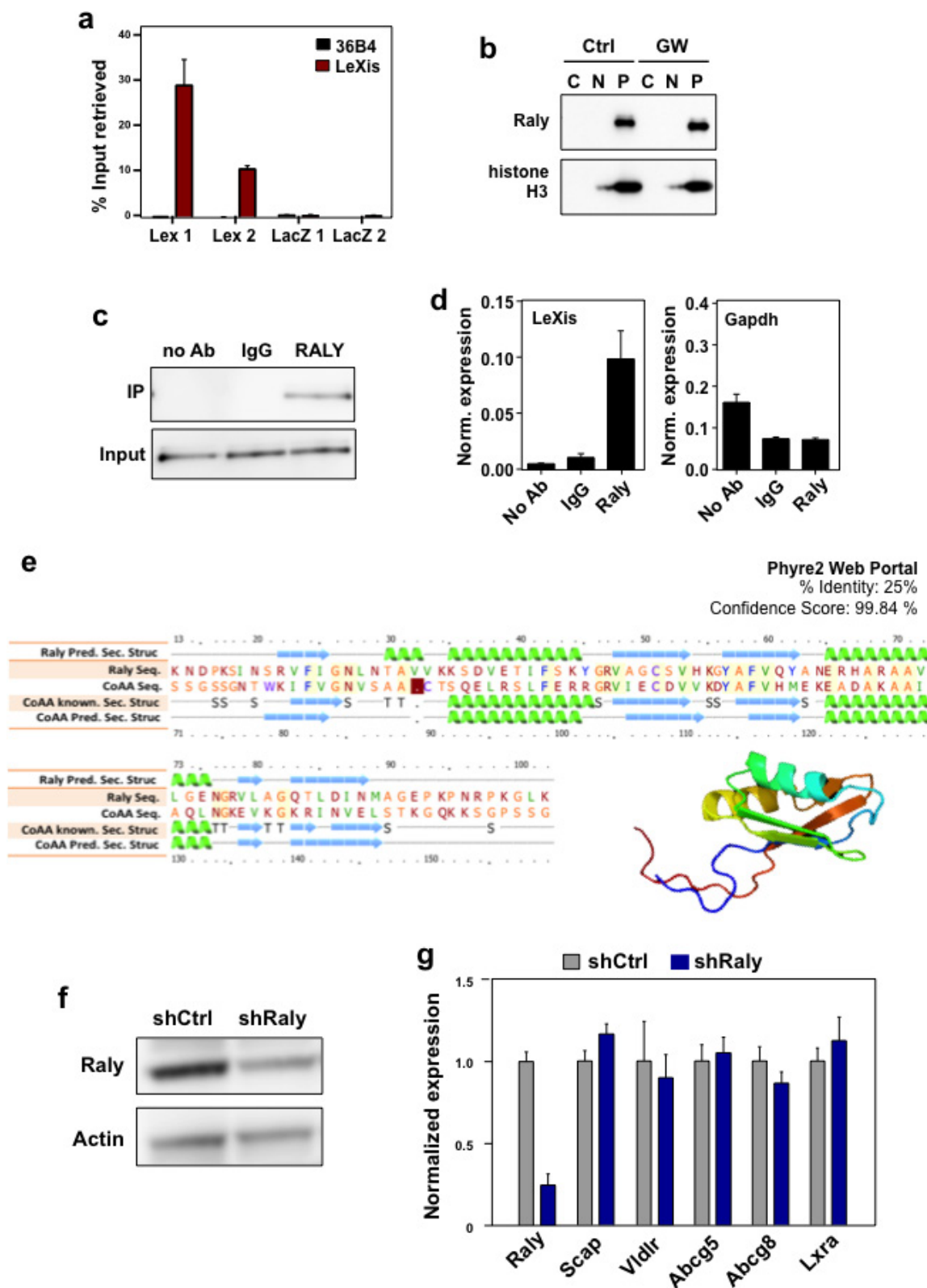
GW3965 for 6 days ($n = 8$ per group). **h**, Gene expression in livers of chow-fed C57BL/6 mice transduced with shCtrl or shLeXis adenovirus and gavaged with 40 mg kg^{-1} GW3965 for 6 days ($n = 8$ per group). **i**, Serum alanine aminotransferase activity from mice in **h**. **j**, Serum alanine aminotransferase activity from mice in **d**. **k**, Gene expression in livers of mice fed a Western diet for 2 weeks and then transduced with shCtrl or shLeXis ($n = 8$ (shCtrl) and 7 (shLeXis1)). **l**, Serum alanine aminotransferase activity from C57BL/6 mice on a chow diet administered 25 mg kg^{-1} ASOs intraperitoneally on days 1, 4 and 7, and gavaged with 40 mg kg^{-1} GW3965 on days 4, 7 and 8 ($n = 5$ per group). **m**, Total serum cholesterol from C57BL/6 mice on a chow diet administered 25 mg kg^{-1} ASOs intraperitoneally on days 1, 3 and 5, and gavaged with 40 mg kg^{-1} GW3965 on days 5 and 6 ($n = 8$ per group). Values are mean \pm s.d. (**a**) or mean \pm s.e.m. (**f**, **h-m**). * $P < 0.05$; ** $P < 0.01$; *** $P < 0.001$ (unpaired two-tailed *t*-test (**b**, **d-h**, **j**) and ANOVA with multi-group comparison (**m**)).



Extended Data Figure 6 | Generation of global *LeXis*^{-/-} mice.

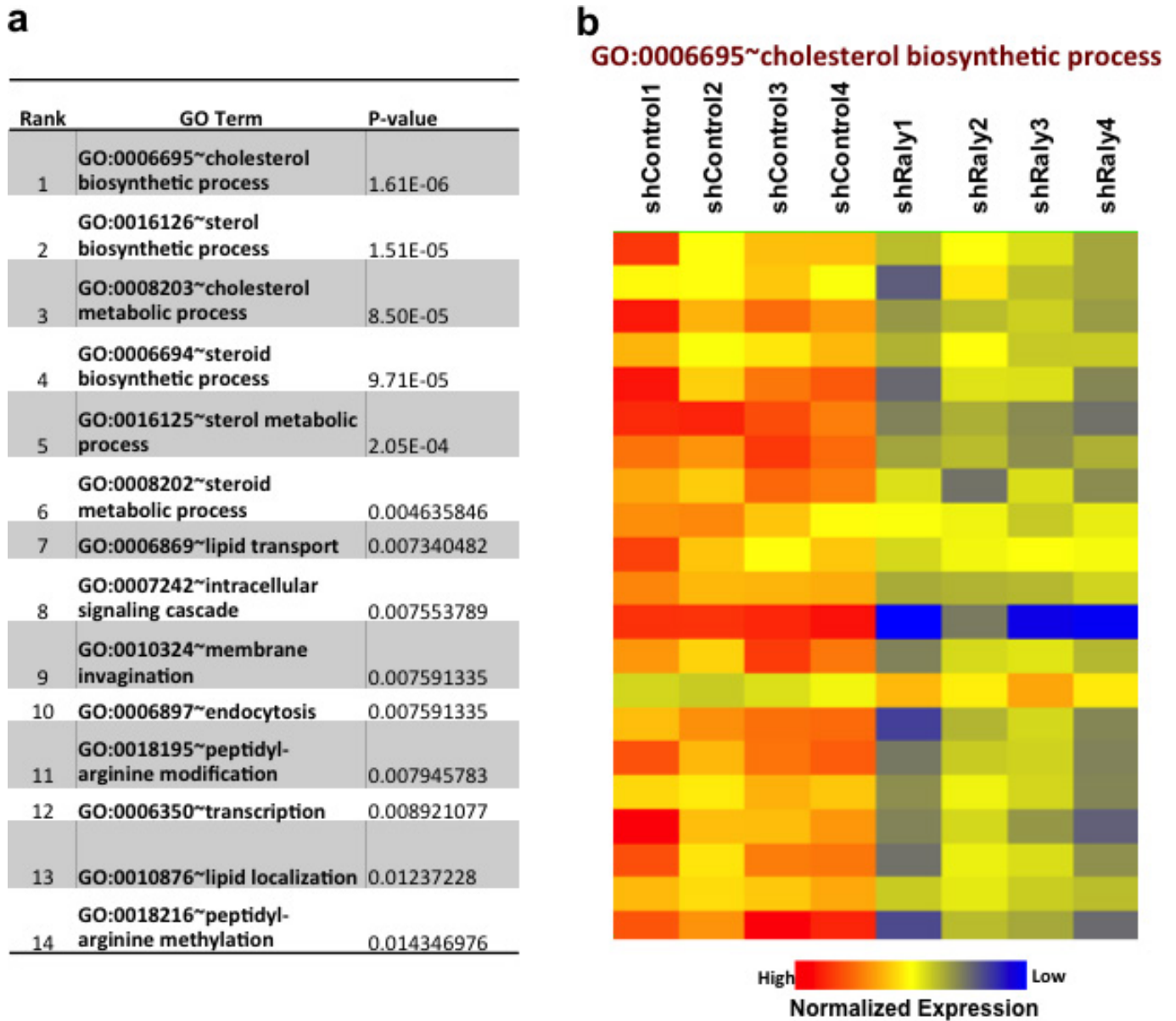
a, Schematic of knockout strategy. Vector construct designed to ablate entire *LeXis* transcript. Targeted mice were crossed with *Flp*^{-/-} (also known as *Hpd*^{-/-}) mice to excise the Neo cassette since it contains an active bi-directional promoter. **b**, **c**, Gene expression ($n = 3$ per group)

and PCR genotyping strategy for *LeXis*^{-/-} mice. **d**, Gene expression from C57BL/6 wild-type or *LeXis*^{-/-} mice fed on Western diet for 3 weeks ($n = 11$ (WT) and 7 (*LeXis*^{-/-})). All values are mean \pm s.e.m. * $P < 0.05$ (unpaired two-tailed *t*-test).

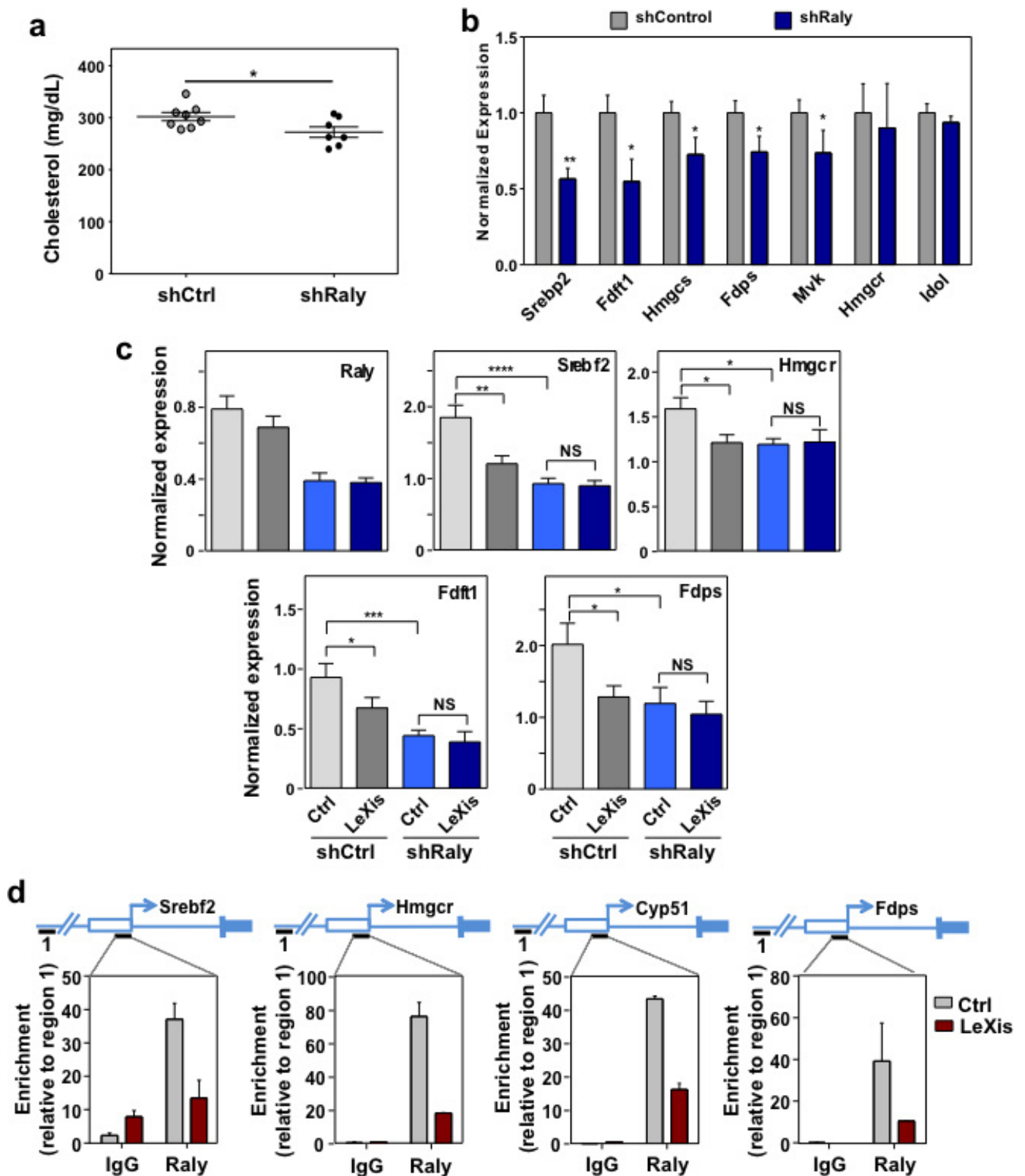


Extended Data Figure 7 | Identification of RALY as a LeXis-interacting protein. **a**, Complimentary biotin-labelled tiling oligonucleotides incubated with cellular extracts from liver. Probes sets designed to retrieve *LeXis* (Lex 1 and 2) or LacZ (LacZ 1 and 2). Percentage input of retrieved *LeXis* and *36B4* are shown ($n = 4$ per group). **b**, Cellular contents separated into cytoplasmic soluble (C), nuclear soluble (N) and insoluble (pellet, P) fractions were analysed by western blotting with anti-RALY and anti-histone H3 antibodies. **c**, Antibodies were incubated with cellular lysates and interaction with endogenous RALY was assessed after immunoprecipitation and western blot. **d**, Complexes from

b were analysed for presence of *LeXis* or *Gapdh* by reverse transcription qPCR (RT-qPCR) and signals were normalized to *36B4* ($n = 4$ per group). **e**, Sequence alignment, predicted secondary structure, and 3D model of RALY are shown as reported using the Phyre2 (Protein Homology/analogue Recognition Engine V 2.0) web portal. **f**, Western blot for RALY from livers transduced with adenoviral vectors expressing control shRNA (shCtrl) or *Raly* shRNA (shRaly) ($n =$ pooled 4 animals per group). **g**, Gene expression from liver from 14-week-old chow-fed male C57BL/6 mice transduced with control (shCtrl) or shRaly ($n = 8$ per group). Values are mean \pm s.d. (**a**) or mean \pm s.e.m. (**g**).

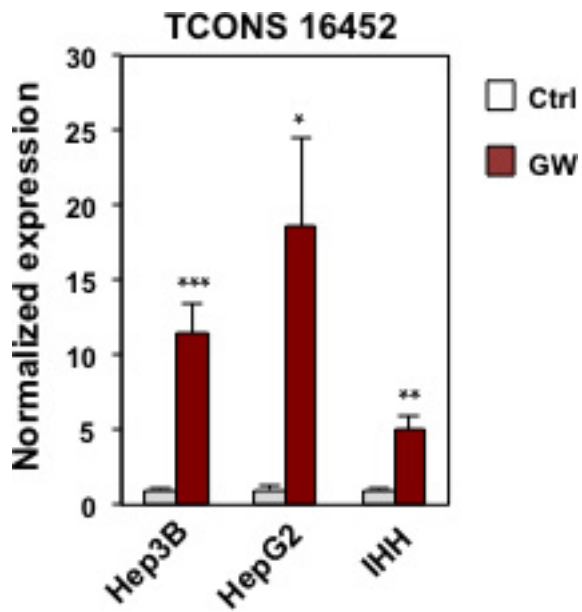


Extended Data Figure 8 | Knockdown of RALY preferentially affects pathways link to cholesterol metabolism in mouse liver. a, b, Most significant Gene Ontology terms from microarray analysis from livers treated with shCtrl or shRaly. Analysis performed using GeneSpring and DAVID.



Extended Data Figure 9 | RALY is required for *LeXis* mediated effects on cholesterologenesis. **a**, Total serum cholesterol levels in *Ldlr*^{-/-} mice transduced with shCtrl or shRaly for 6 days ($n = 8$ (shCtrl) and 7 (shRaly)). **b**, Gene expression from liver obtained from *Ldlr*^{-/-} mice transduced with shCtrl or shRaly for 6 days ($n = 8$ (shCtrl) and 7 (shRaly)). **c**, Gene expression from C57BL/6 mice transduced with control (Ad-GFP) or Ad-*LeXis* (1.0×10^9 p.f.u.) and shCtrl or shRaly (2.0×10^9 p.f.u.) ($n = 7$

(ctrl/shCtrl and *LeXis*/shRaly) and 8 (*LeXis*/shCtrl and Ctrl/shRaly)). **d**, Recruitment of RALY in promoter regions as determined by ChIP analysis in livers transduced with control (Ad-GFP) or Ad-*LeXis*. Data expressed as percentage input retrieved normalized to an upstream site (region 1) ($n = 3$ per group). Values are mean \pm s.e.m. (**b**, **c**) or mean \pm s.d. (**d**). * $P < 0.05$; ** $P < 0.01$; *** $P < 0.001$; **** $P < 0.0001$ (unpaired two-tailed *t*-test (**a**, **b**) and ANOVA with multi-group comparison (**c**)).



Extended Data Figure 10 | Batch genome conversion between mouse and human at *LeXis* gene locus. Gene expression for putative human non-coding RNA TCONS_00016452 in hepatocyte cell lines treated with 1 μ M GW3965 ($n = 3$ per group). Values are mean \pm s.d. * $P < 0.05$; ** $P < 0.01$; *** $P < 0.001$ (unpaired two-tailed t -test).